International Journal of Mechanical, Industrial and Aerospace Sciences
ISSN: 2517-9950
Vol:10, No:7, 2016

Numerical Analysis of the Melting of Nano-Enhanced Phase Change Material in a Rectangular Latent Heat Storage Unit

Radouane Elbahjaoui, Hamid El Qarnia

***Abstract*—**Melting of Paraffin Wax (P116) dispersed with Al_2O_3 nanoparticles in a rectangular latent heat storage unit (LHSU) is numerically investigated. The storage unit consists of a number of vertical and identical plates of nano-enhanced phase change material (NEPCM) separated by rectangular channels in which heat transfer fluid flows (HTF: Water). A two dimensional mathematical model is considered to investigate numerically the heat and flow characteristics of the LHSU. The melting problem was formulated using the enthalpy porosity method. The finite volume approach was used for solving equations. The effects of nanoparticles' volumetric fraction and the Reynolds number on the thermal performance of the storage unit were investigated.

***Keywords*—**Nano-enhanced phase change material, phase change material, nanoparticles, latent heat storage unit, melting.

I. Introduction

DUE to the high energy storage capacity, LHSUs using phase change materials (PCMs) have gained great attention over the last three decades. However, PCMs are characterized by a low thermal conductivity, which limits the heat exchange rate and slowed the melting/solidification rate of these materials. To overcome this drawback and improve the heat transfer rate during the solid-liquid phase change process, several methods have been suggested in the literature. These methods include the dispersion of nanoparticles with a very high conductivity in PCMs [1], integration of metal matrix in PCMs [2], use of multiple PCMs [3], [4] and porous matrix [5]. Among these methods, dispersion of high conductivity nanoparticles in PCM is the main topic of this study.

In recent years, a number of experimental and numerical works have been performed to investigate the thermal performance of NEPCM. Khodadadi and Hosseinizadeh [6] were the first who studied numerically the improving of the functionality of phase change material (PCM: water) by dispersion of nanoparticles (copper) during the solidification process with natural convection in a square cavity. The results of this study showed that NEPCM releases heat quickly compared to a basic PCM. Ho and Gao [7] experimentally studied the melting in a square enclosure filled with PCM (n-octadecane) with dispersed nanoparticles (Al_2O_3). They reported that the influence of the solid subcooling through the un-melted PCM can be further enhanced by dispersion of high conductivity nanoparticles in the enclosure. They also indicated that natural convection heat transfer in the liquid region degrades significantly with the increase of the mass fraction of nanoparticles when compared with natural convection corresponding to a base PCM. Sebti et al. [8] conducted a 2D numerical study to investigate heat transfer enhancement over melting process in a square enclosure through dispersion of nanoparticles. Authors reported that the dispersion of nanoparticles causes a decrease of the melting time. They also reported that the increase of the difference between the melting point and the hot wall temperature leads to a significant decrease of the melting time. Hossain et al. [9] developed a two dimensional thermal model to study the melting process of NEPCM inside a rectangular porous medium. The results show that the NEPCM melts rapidly within the lower porosity medium. Shuja et al. [10] performed experimental and numerical investigations of the thermal characteristics of PCM (n-octadecane) integrated with metallic meshes. They examined the effect of the mesh geometry on the melting time for two different metallic mesh arrangements. The results show that the melting time of PCM is the shortest for the triangular mesh geometry then followed by the rectangular and hexagonal mesh. Sciacovelli et al. [11] conducted a numerical analysis of the melting of NEPCM in a shell-and-tube LHSU. They demonstrate that the melting time is reduced by 15% when the PCM is dispersed with nanoparticles volume fraction of 4%. Kashani et al. [12] numerically studied the effects of nanoparticles volume fraction and the cold wall temperature during the solidification of NEPCM filled in a rectangular enclosure. They found that a large solid fraction is obtained for a smaller wall temperature and a high nanoparticle volume fraction. Hosseinizadeh et al. [13] conducted a numerical study of the melting of NEPCM inside a spherical container. The simulation results of this study show a pronounced potential of using PCM with dispersed nanoparticles. Jourabian et al. [14] numerically examined the melting of Cu/water NEPCM inside a cylindrical horizontal annulus by using the enthalpy-based lattice Boltzmann method. Their results show that owing to the enhancement of thermal conductivity, the effect of volume fraction of nanoparticles on heat transfer rate is more significant. Their results also indicate that the temperature distribution in the NEPCM is faster than that of base PCM.

To the authors' knowledge, there are no comprehensive

El Qarnia, H. and Elbahjaoui, R. are with the Cadi Ayyad University, Faculty of Science Semlalia, Department of Physics, Fluid Mechanics and Energetic Laboratory, Marrakesh, B.P. 2390, Morocco (phone: +212 666350016, e-mail: elqarnia@uca.ac.ma).

studies published in the literature for melting of NEPCM in rectangular enclosures heated by laminar forced convection. In the present work, the modeling and numerical investigation of a LHSU composed of several vertical slabs filled with Al_2O_3/Paraffin Wax is presented. A laminar heat transfer fluid flow (water) circulates between the Nano-enhanced PCM slabs and transfers heat to the storage unit. The objective of the present study is to investigate the effects of nanoparticles volumetric fraction and the Reynolds number on the thermal behaviour and performance of the storage unit.

II. Problem Formulation

A. Description of the Studied Physical Model

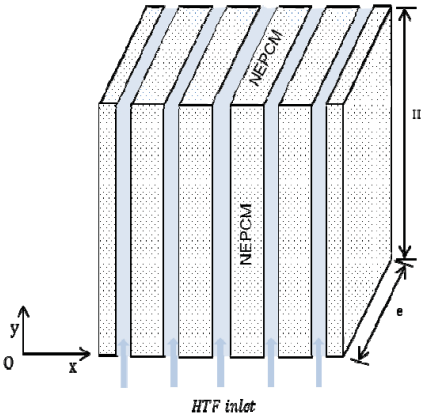

Fig. 1 (a) LHSU

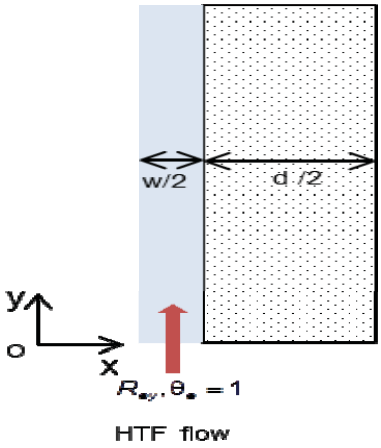

Fig. 1 (b) Computational domain

The present LHSU is illustrated in Fig. 1 (a). It is composed of a number of vertical and identical plates filled with NEPCM (Al_2O_3/P116). A heat transfer fluid (HTF: water) flows between the plates and transfers heat by laminar forced convection to NEPCM. For reasons of symmetry of the storage unit, the study of overall system can be reduced to the study of a half NEPCM plate and a half HTF channel as illustrated in Fig. 1 (b). The height and thickness of the rectangular NEPCM plates are H and d, respectively. The thickness of the HTF channels is w.

Initially, the plates contain solid NEPCM at a temperature equal to the melting temperature, T_0. At t >0, the HTF begins to flow between the NEPCM plates, which triggers the melting process. The water inlet temperature to the storage unit is fixed at a constant value higher than the melting point.

B. Governing Equations

The modeling of the thermal and flow characteristics of the LHSU is performed by using the governing conservation equations of energy for HTF, continuity, momentum and energy equations for NEPCM. The flow in HTF channels and liquid NEPCM is laminar and two-dimensional. The HTF and liquid phase of PCM are incompressible and Newtonian. For the HTF (water) circulating in channels, the flow is assumed hydro-dynamically fully developed. The thermo-physical properties are assumed to be constant except for the density difference according to the Boussinesq approximation. The enthalpy–porosity approach was used for the formulation of phase change problem.

The density of NEPCM is given by:

$$\rho_{nm} = \phi\rho_n + (1-\phi)\rho_m \tag{1}$$

The specific heat and Boussinesq term of the NEPCM are defined as:

$$(\rho c_p)_{nm} = \phi(\rho c_p)_n + (1-\phi)(\rho c_p)_m \tag{2}$$

$$(\rho\beta)_{nm} = (1-\phi)(\rho\beta)_m + \phi(\rho\beta)_n \tag{3}$$

The latent heat of the NEPCM is evaluated as [15]:

$$(\rho\Delta H)_{nm} = (1-\phi)(\rho\Delta H)_m \tag{4}$$

where ϕ is the nanoparticles volumetric fraction and subscripts n, m and nm stand for nanoparticles, PCM and NEPCM, respectively. The viscosity of the NEPCM containing a small spherical suspension of solid particles is given as:

$$\mu_{nm} = \frac{\mu_m}{(1-\phi)^{2.5}} \tag{5}$$

whereas the thermal conductivity of the NEPCM is defined by:

$$k_{nm} = k_{eff} + k_d \tag{6}$$

where k_{eff} is the thermal conductivity of the stagnant NEPCM and k_d corresponds to the conductivity enhancement term which represents the Brownian motion. They are considered as:

$$k_{eff} = \frac{k_n + 2k_m - 2(k_m - k_n)\phi}{k_n + 2k_m + (k_m - k_n)\phi} k_m \tag{7}$$

$$k_d = C^*(\rho c_p)_{nm}\sqrt{u^2+v^2}\,d_n \quad (8)$$

where d_n is the diameter of nanoparticles (d_n = 45 nm) and C^* is an empirical constant evaluated according to [16].

The governing equations are converted in dimensionless form using the following parameters:

$$X=\frac{x}{l_0}, Y=\frac{y}{l_0}, \tau=\frac{\alpha_{m,l}\,t}{l_0^2}, U=\frac{u}{\alpha_{m,l}/l_0}, V=\frac{v}{\alpha_{m,l}/l_0},$$
$$\Delta T = T_{fe}-T_o, \theta=\frac{T-T_o}{T_{fe}-T_o}, Ra=\frac{g\beta_m l_0^3 \Delta T}{\upsilon_m \alpha_{m,l}},$$
$$Pr=\frac{\upsilon_{nm}}{\alpha_{nm,l}}, P=\frac{p}{\rho_{nm}(\alpha_{m,l}/l_0)^2}, \bar{\alpha}=\frac{\alpha}{\alpha_{m,l}},$$
$$Ste=\frac{c_{nm}\Delta T}{\Delta H_{nm}}, \bar{w}=\frac{w}{l_0}, \bar{d}=\frac{d}{l_0}, \bar{H}=\frac{H}{l_0},$$
$$\bar{k}_f=\frac{k_f}{k_{m,l}} \text{ and } \bar{k}_{nm}=\frac{k_{nm}}{k_{m,l}}$$

where T_{fe} is the HTF inlet temperature, T_0 is the melting temperature, Ra is the Rayleigh number, Ste is the Stefan number and l_0 is the characteristic length ($l_0=\sqrt{H\,d/2}$). Based on these dimensionless numbers, the set of governing equations are written as:

For HTF,

$$\frac{\partial\theta_f}{\partial\tau}+\frac{\partial(V_f\theta_f)}{\partial Y}=\frac{\partial}{\partial X}\left(\bar{\alpha}_f\frac{\partial\theta_f}{\partial X}\right)+\frac{\partial}{\partial Y}\left(\bar{\alpha}_f\frac{\partial\theta_f}{\partial Y}\right) \quad (9)$$

For NEPCM, Continuity:

$$\frac{\partial U}{\partial X}+\frac{\partial V}{\partial Y}=0 \quad (10)$$

Momentum:

$$\frac{\partial U}{\partial\tau}+\frac{\partial UU}{\partial X}+\frac{\partial VU}{\partial Y}=-\frac{\partial P}{\partial X} + \frac{\partial}{\partial X}\left(Pr\,\bar{\alpha}_{nm,l}\frac{\partial U}{\partial X}\right)+\frac{\partial}{\partial Y}\left(Pr\,\bar{\alpha}_{nm,l}\frac{\partial U}{\partial Y}\right)+\bar{S}_u \quad (11)$$

$$\frac{\partial V}{\partial\tau}+\frac{\partial UV}{\partial X}+\frac{\partial VV}{\partial Y}=-\frac{\partial P}{\partial Y}+\frac{\partial}{\partial X}\left(Pr\,\bar{\alpha}_{nm,l}\frac{\partial V}{\partial X}\right) + \frac{\partial}{\partial Y}\left(Pr\,\bar{\alpha}_{nm,l}\frac{\partial V}{\partial Y}\right)+\bar{S}_v \quad (12)$$

Energy:

$$\frac{\partial(\theta_{nm})}{\partial\tau}+\frac{\partial(U\theta_{nm})}{\partial X}+\frac{\partial(V\theta_{nm})}{\partial Y}=\frac{\partial}{\partial X}\left(\bar{\alpha}_{nm}\frac{\partial\theta_{nm}}{\partial X}\right) + \frac{\partial}{\partial Y}\left(\bar{\alpha}_{nm}\frac{\partial\theta_{nm}}{\partial Y}\right)+\bar{S}_h \quad (13)$$

C. Boundary and Initial Condition

The initial and boundary conditions of the present computational domain are given by the following relations:

$$\tau=0: \quad \theta_{nm}=\theta_f=0,\ U=V=0 \quad (14)$$

$$X=0: \quad \frac{\partial\theta_f}{\partial X}=0 \quad (15)$$

$$X=\bar{w}/2: \quad \bar{k}_f\frac{\partial\theta_f}{\partial X}=\bar{k}_{nm}\frac{\partial\theta_{nm}}{\partial X},\ U=V=0 \quad (16)$$

$$Y=0: \quad \theta_f=1,\ \frac{\partial\theta_{nm}}{\partial Y}=0,\ U=V=0 \quad (17)$$

$$X=\bar{w}/2+\bar{d}/2: \quad \frac{\partial\theta_{nm}}{\partial Y}=0,\ U=0,\frac{\partial V}{\partial X}=0 \quad (18)$$

$$Y=\bar{H}: \quad \frac{\partial\theta_f}{\partial Y}=\frac{\partial\theta_{nm}}{\partial Y}=0,\ U=V=0 \quad (19)$$

III. Results and Discussions

Numerical simulations were carried out to investigate the thermal behavior and performance of the NEPCM storage unit heated by laminar forced HTF flow. The HTF, PCM and nanoparticles used in the calculations are water, Paraffin Wax P116 and alumina (Al_2O_3), respectively. Their corresponding thermal properties are summarized in Table I. The effects of nanoparticles volumetric fraction, ϕ, and the Reynolds number, Re, on the flow and thermal characteristics of the LHSU were examined. The other governing parameters such as the aspect ratio of the NEPCM slabs, the Rayleigh number, Ra, the dimensionless HTF channels thickness, $\bar{w}$, the LHSU depth, $\bar{e}$, and the characteristic length, l_0, are fixed at values 6, 7.95×10^7, 0.085, 14.16 and 0.07062 m, respectively

TABLE I
Thermal Properties of HTF, PCM and Nanoparticles

Property	HTF (water)	Paraffin Wax P116	Alumina (Al_2O_3)
Density (kg/ m^3)	989	802	3600
Specific heat (J/ kg K)	4180	2510	765
Thermal conductivity (W/ m K)	0.64	0.36(l),0.24(s)	36
Dynamic viscosity (kg/ m s)	577×10^{-6}	1.3×10^{-3}	-
Latent heat (kJ/ kg)	-	226	-
Melting temperature (° C)	-	47	-

In order to investigate numerically the thermal behavior and performance of the NEPCM storage unit heated by laminar HTF flow, two kinds of storage efficiencies were defined. The first concerns the storage of thermal energy by sensible heat. It is expressed as the ratio between the sensible energy stored in NEPCM storage unit and the maximum energy (latent and sensible energy) that can be stored. It is given as:

$$\varepsilon_{sen}=\frac{Ste\int_{X=\bar{w}/2}^{\bar{w}/2+\bar{d}/2}\int_{Y=0}^{\bar{H}}\theta_{nm}\,dX\,dY}{1+Ste} \quad (20)$$

The second kind of efficiency concerns the energy storage by latent heat. It is defined as the ratio between the latent heat stored and the maximum energy that can be charged in

NEPCM. It is expressed as:

$$\varepsilon_{lat} = \frac{f}{1 + Ste} \quad (21)$$

A. Effect of Volume Fraction on the Streamlines and Isotherms

The streamlines describing the flow field in the liquid NEPCM at different times: 0.0215, 0.0487, 0.072 and 0.123 for nanoparticles volumetric fraction, $\phi = 0$ % and $\phi = 6\%$, are shown in Figs. 2 (a)-(d) and 3 (a)-(d), respectively, with A = 16, Re = 1000 and Ra = 7.95×10^7. With the start of HTF circulation between the NEPCM slabs, a part of the heat lost by HTF is transmitted to NEPCM thereby causing the beginning of melting. These figures show that natural convection begins to settle near the heat exchange wall separating HTF and NEPCM. Clockwise cells of ascending warm and descending cold liquid are created in the NEPCM liquid. The heated NEPCM liquid moves up toward the top part of slabs before impinging on the solid-liquid interface. At the beginning of the melting process, the effect of natural convection is generally weak and the main heat transfer mode is thermal conduction. At $\tau = 0.0215$, the NEPCM liquid flow is mono-cellular and the flow intensity is substantially the same for both cases of volumetric fraction of nanoparticles ($\Psi_{min} = -80$). As time progresses, the effect of natural convection becomes more important which affects the morphology of the solid-liquid interface. For both cases of volumetric fractions of nanoparticles, the displacement of the hot NEPCM liquid towards the top portion of the slabs causes an accelerated melting in this region. With the progress of time ($\tau = 0.0487$ and 0.072), the clockwise cells formed widens in volume and the convective flow appears more intensified for 0% (Ψ_{min} = -120 and -100 at τ = 0.0487 and 0.072, respectively). At $\tau = 0.132$, the whole NEPCM has become liquid where the streamlines covered the entire slabs. It should be noted that for both cases of nanoparticles' volumetric fractions, the central cells previously formed occupy the entire slab.

The temperature distributions in NEPCM liquid for ϕ = 0% at the same times: 0.0215, 0.0487, 0.072 and 0.123 are shown in Figs. 4 (a)-(d) with A = 16, Re = 1000. For ϕ = 6%, the temperature distributions in liquid NEPCM are illustrated in Figs. 5 (a)-(d). At the early stages, the heat transfer within NEPCM is controlled by thermal conduction and therefore the isotherms are almost in alignment with the y-axis. As time progresses, natural convection start to affect the melting process and the NEPCM liquid begins to occupy a substantial portion of the slab. For both cases of nanoparticles' volumetric fractions, the heated liquid phase in contact with the exchange wall moves up toward the upper part of the slab which causes deformation of temperature contours. So, the maximum temperature is reached in the upper part of the NEPCM slab. These figures also show that the greatest temperature gradients are found close to the heat exchange wall while vertical temperature gradients are observed in the region where the eddy is located. It should be noted that the comparison between Figs. 4 and 5 shows that, at the same time, the maximum temperature is achieved for the case of $\phi = 6\%$.

A. Effect of the Reynolds Number

The effect of the Reynolds number, Re, on the time wise variation of the sensible storage efficiency, for different volumetric fractions of nanoparticles, is illustrated in Fig. 6 for A = 6 and Ra= $7.95\text{x}10^7$. As can be seen in this figure, the sensible storage efficiency increases nonlinearly to reach its maximum when the thermal equilibrium is established between HTF and NEPCM. The maximum value of the sensible storage efficiency is about 0.126, 0.129 and 0.139 for ϕ = 0%, 2% and 8%, respectively. This figure also shows that the charging time of the storage unit decreases with the increase of the volumetric fraction of nanoparticles dispersed in PCM. Therefore, the sensible heat is early stored in NEPCM for a high nanoparticles' volumetric fraction. It can be also concluded that the increase of the Reynolds number leads to a decrease in the charging time. Indeed, the increase of the Reynolds number intensifies heat transfer between HTF and NEPCM through the exchange surface.

The effect of the Reynolds number on the time wise variation of the latent storage efficiency, for several volumetric fractions of nanoparticles, is shown in Fig. 7. The aspect ratio of the NEPCM slabs is A = 6 and the Rayleigh number is Ra = $7.95\text{x}10^7$. The results reveal that the latent storage efficiency reaches its maximum value very quickly when the Reynolds number increases which causes a decrease of the time required for the complete melting. It should be noted that this maximum value of the latent storage efficiency decreases with the increase of the volumetric fraction of NEPCM. This result is due to the fact that the dispersion of nanoparticles in pure PCM leads to the diminution of the volumetric fraction of pure PCM in NEPCM slabs.

The effect of the Reynolds number on the time required for complete melting is shown in Figs. 8 (a), (b) for A = 6 and 16, respectively. As concluded in the previous section, the melting time decreases with the increase of the Reynolds number. These figures show that for all Reynolds numbers and for both cases of NEPCM aspect ratio, the melting time is smaller for a high volumetric fraction of nanoparticles.

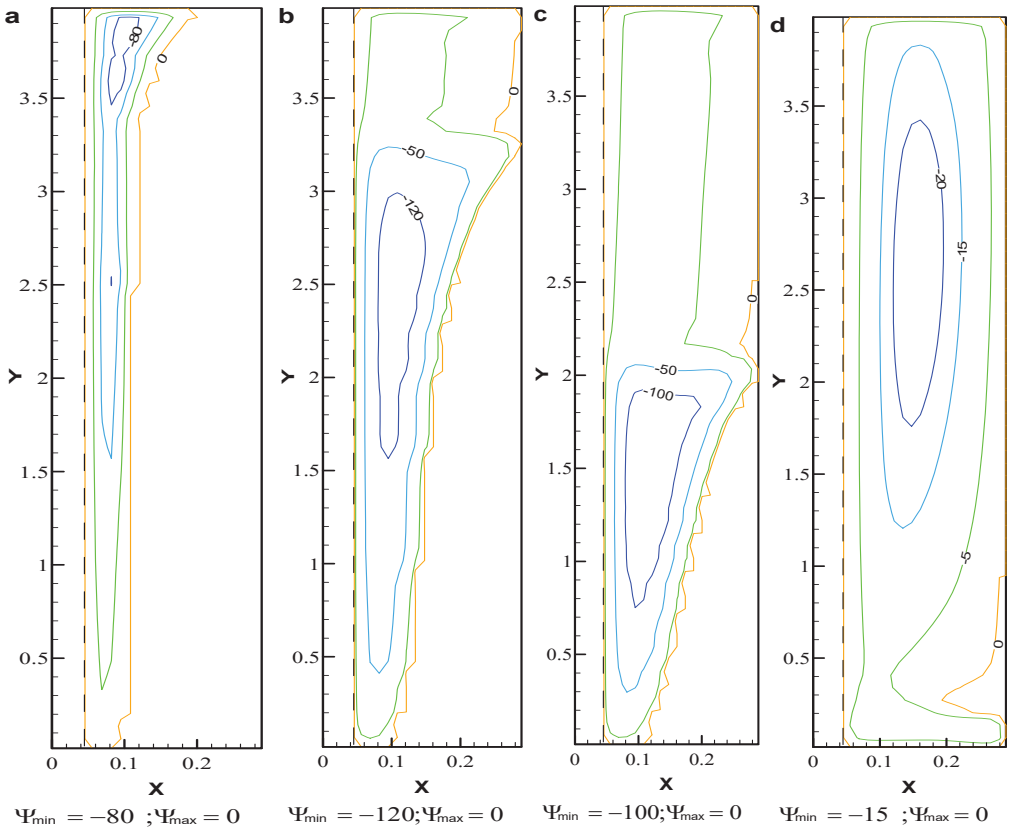

Fig. 2 Streamlines for ϕ=0% at (a) $\tau = 0.0215$, (b) 0.0487, (c) 0.072 and (d) 0.132 with A=16, Re=1000 and Ra=7.95x10^7

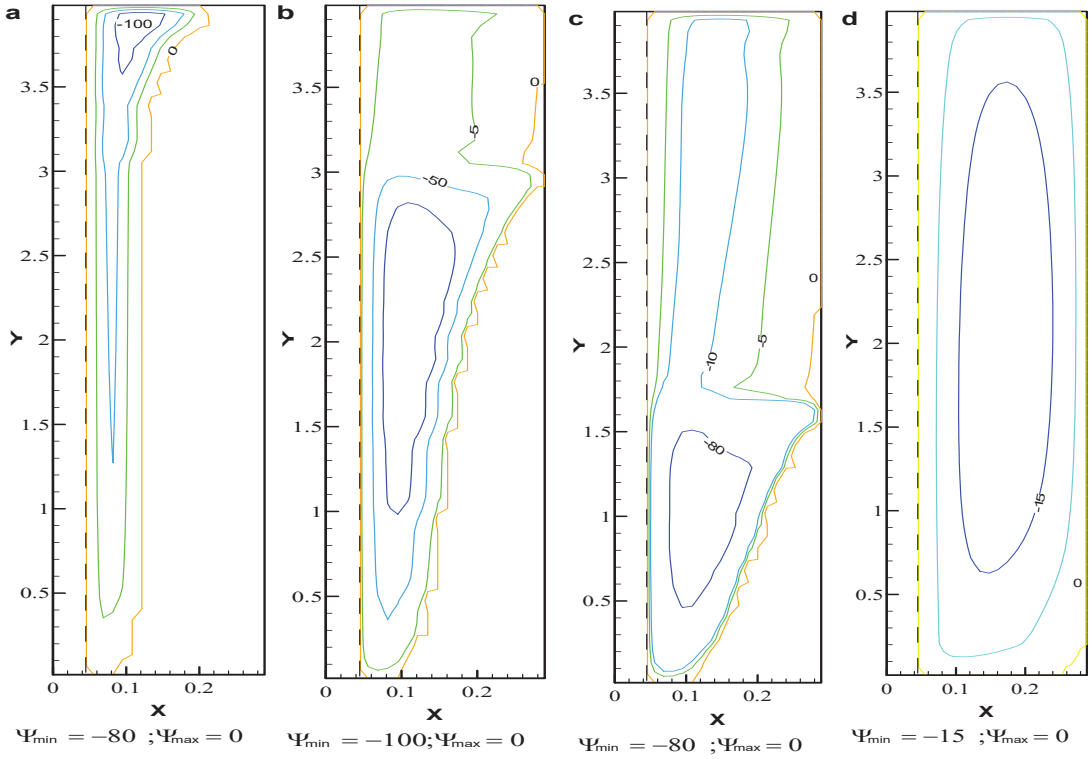

Fig. 3 Streamlines for ϕ=6% at (a) $\tau = 0.0215$, (b) 0.0487, (c) 0.072 and (d) 0.132 with A=16, Re=1000 and Ra=7.95x10^7

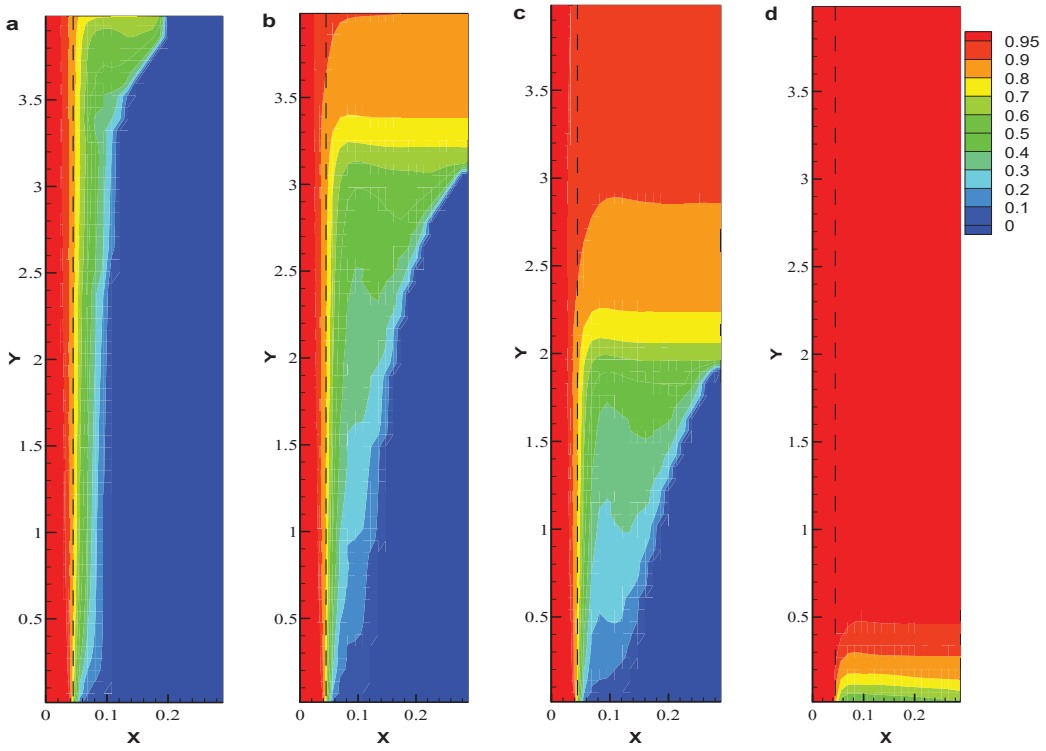

Fig. 4 Isotherms for ϕ=0% at (a) $\tau = 0.0215$, (b) 0.0487, (c) 0.072 and (d) 0.132 with A=16, Re=1000 and Ra=7.9510^7

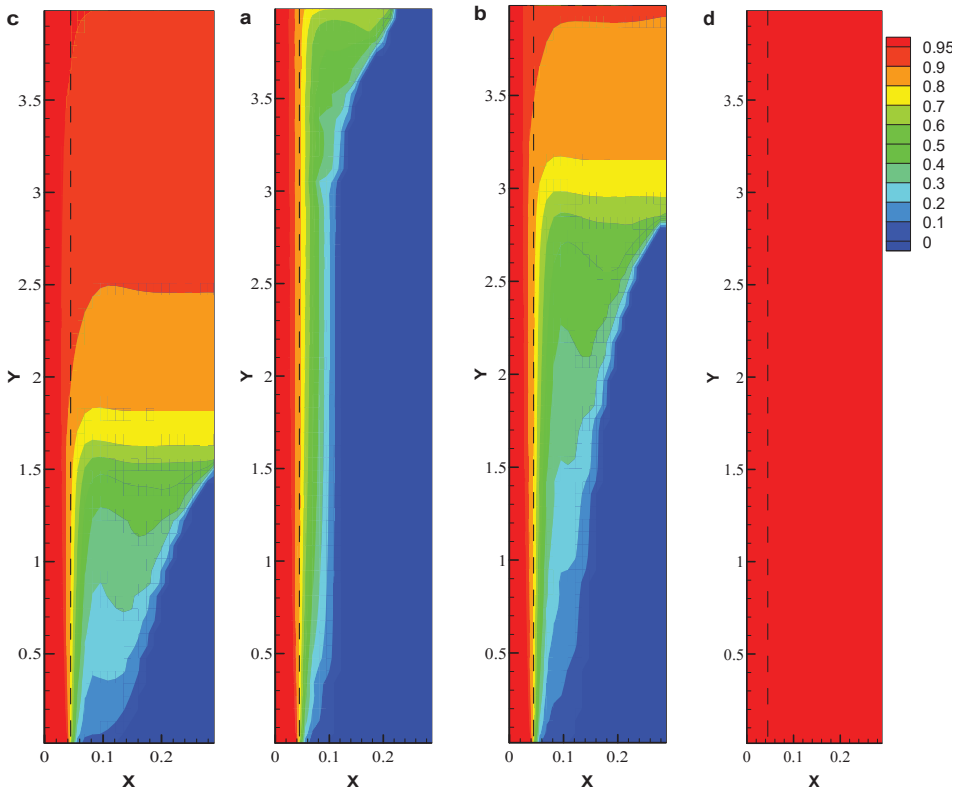

Fig. 5 Isotherms for ϕ=6% at (a) $\tau = 0.0215$, (b) 0.0487, (c) 0.072 and (d) 0.132 with A=16, Re=1000 and Ra=7.9510^7

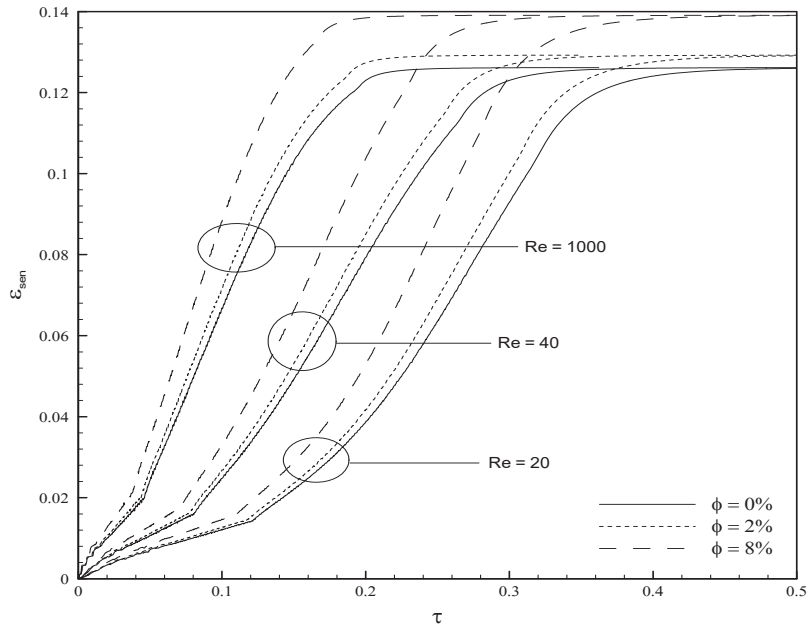

Fig. 6 Effect of the Reynolds number on the time wise variation of the sensible storage efficiency for various volumetric fractions of nanoparticles with A = 6 and Ra=7.95x10^7

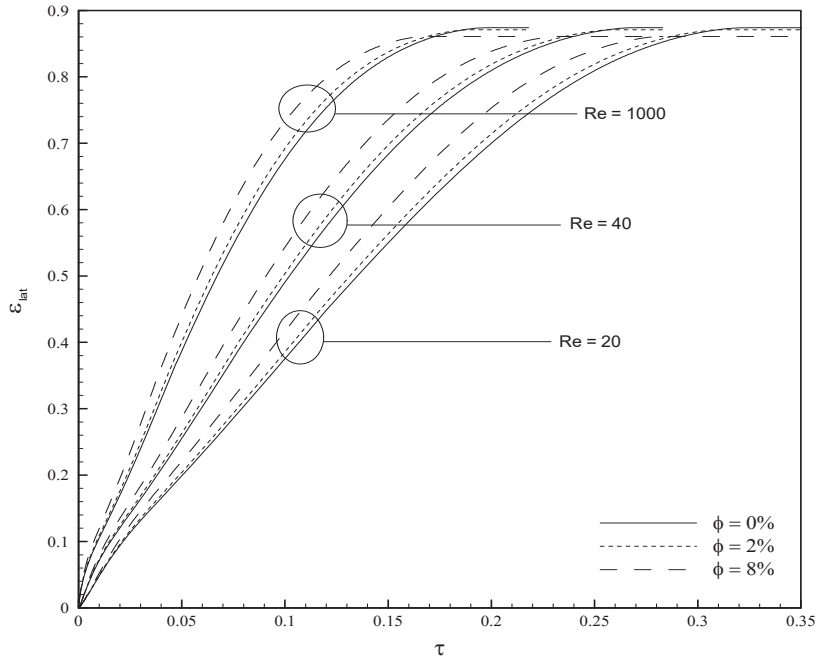

Fig. 7 Effect of the Reynolds number on the time wise variation of the latent storage efficiency for various volumetric fractions of nanoparticles with A = 6 and Ra=7.9510^7

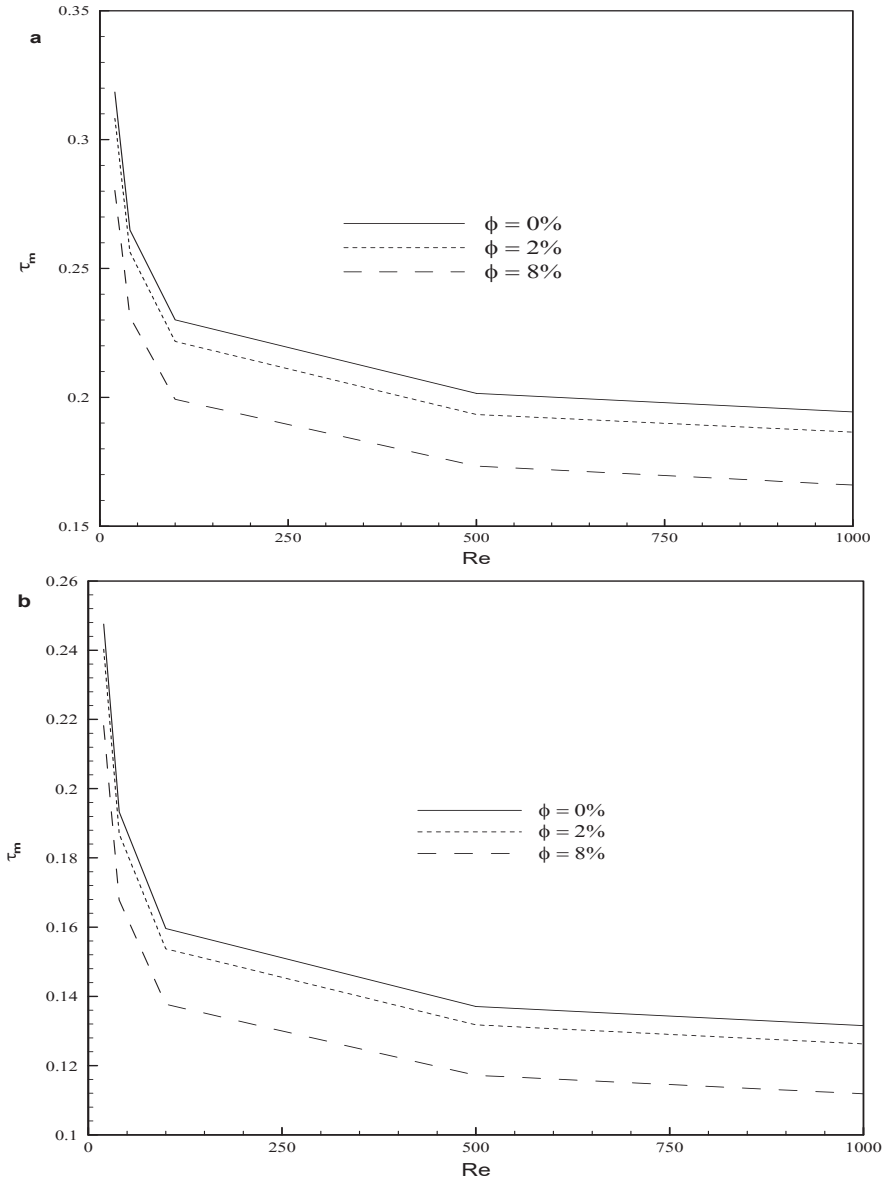

Fig. 8 Effect of the Reynolds number on the melting time for various volumetric fractions of nanoparticles for (a) A = 6 and (b) A = 16 with Ra = 7.95×10^7

IV. Conclusion

In the present research, melting of NEPCM in a rectangular LHSU heated with laminar heat transfer fluid flow has been studied numerically. A mathematical model based on the conservation equations of mass, momentum and energy has been elaborated to investigate the effect of the volumetric fraction of nanoparticles dispersed in pure PCM and the aspect ratio of the NEPCM plates on the thermal performance of the LHSU.

Based on the findings of the present computational study, the following conclusions are drawn:

- The dispersion of high conductivity nanoparticles in a pure PCM causes the decrease in the melting time;
- The increase in the volumetric fraction of nanoparticles ($\phi \leq 8\%$) increases the sensible storage efficiency and slightly affects the latent storage efficiency;
- The increase in the Reynolds number intensifies heat exchange between HTF and NEPCM and decreases the time required for the complete melting.

Nomenclature

Symbol	Quantity
A	Aspect ratio, H/ (d/2)
c	Specific heat at constant pressure (J/kg K)
d	PCM slabs thickness (m)
f	Liquid fraction
g	Gravity (m/s2)
h	Volumetric enthalpy (J/m3)

H	Height of the PCM slabs (m)
k	Thermal conductivity (W/ m.K)
$\bar{k}$	Dimensionless thermal conductivity, k/km,l
p	Pressure (N/m2)
Ra	Rayleigh number
Ste	Stefan number
T	Temperature (K)
t	time (s)
u, v	velocity components (m/ s)
x,y	Cartesian coordinates (m)
w	thickness of the HTF channels (m)

Greek Symbols

α	Thermal diffusivity (m2/s)
$\bar{\alpha}$	Dimensionless thermal diffusivity, $\alpha/\alpha_{m,l}$
ϕ	Volumetric fraction of nanoparticles
β	coefficient of thermal expansion of liquid PCM (K-1)
θ	Dimensionless temperature
τ	dimensionless time
μ	dynamic viscosity (N.s/m3)
ν	kinematic viscosity (m2/s)
ΔH	latent heat (J/ kg)
ρ	density (kg/ m3)
ε	storage efficiency
Ψ	dimensionless stream function

Subscripts

e	Inlet
f	Heat transfer fluid (HTF)
l	Liquid
lat	Latent
nm	Nano-enhanced phase change material (NEPCM)
m	PCM
o	Outlet

Non-dimensional Numbers

Re	Reynolds number
Ra	Rayleigh number
Ste	Stefan number

REFERENCES

[1] T. Li and Y. V. Rogovchenko, "Asymptotic Behavior of Higher-Order Quasilinear Neutral Differential Equations," Abstract and Applied Analysis, 2014, p. 11.

[2] J. A. K. Xinglin Tong, M. RuhulAmin, "Enhancement of heat transfer by inserting a metal matrix into a phase change material,"

[3] H. Ait Adine and H. El Qarnia, "Numerical analysis of the thermal behaviour of a shell-and-tube heat storage unit using phase change materials," Applied Mathematical Modelling, 2009, pp. 2132-2144.

[4] Y. Tian and C. Y. Zhao, "Thermal and exergetic analysis of Metal Foam-enhanced Cascaded Thermal Energy Storage (MF-CTES)," International Journal of Heat and Mass Transfer, 2013, pp. 86-96.

[5] J. M. Marín, B. Zalba, L. F. Cabeza, and H. Mehling, "Improvement of a thermal energy storage using plates with paraffin–graphite composite," International Journal of Heat and Mass Transfer, 2005, pp. 2561-2570.

[6] J. M. Khodadadi and S. F. Hosseinizadeh, "Nanoparticle-enhanced phase change materials (NEPCM) with great potential for improved thermal energy storage," International Communications in Heat and Mass Transfer, 2007, pp. 534-543.

[7] C. J. Ho and J. Y. Gao, "An experimental study on melting heat transfer of paraffin dispersed with Al2O3 nanoparticles in a vertical enclosure," International Journal of Heat and Mass Transfer, 2013, pp. 2-8.

[8] S. Sebti, M. Mastiani, H. Mirzaei, A. Dadvand, S. Kashani, and S. Hosseini, "Numerical study of the melting of nano-enhanced phase change material in a square cavity," Journal of Zhejiang University SCIENCE A, 2013, pp. 307-316.

[9] R. Hossain, S. Mahmud, A. Dutta, and I. Pop, "Energy storage system based on nanoparticle-enhanced phase change material inside porous medium," International Journal of Thermal Sciences, 2015, pp. 49-58.

[10] S. Z. Shuja, B. S. Yilbas, and M. M. Shaukat, "Melting enhancement of a phase change material with presence of a metallic mesh," Applied Thermal Engineering, 2015, pp. 163-173.

[11] A. Sciacovelli, F. Colella, and V. Verda, "Melting of PCM in a thermal energy storage unit: Numerical investigation and effect of nanoparticle enhancement," International Journal of Energy Research, 2013, pp. 1610-1623.

[12] S. Kashani, A. A. Ranjbar, M. M. Madani, M. Mastiani, and H. Jalaly, "Numerical study of solidification of a nano-enhanced phase change material (NEPCM) in a thermal storage system," Journal of Applied Mechanics and Technical Physics, 2013, pp. 702-712.

[13] S. F. Hosseinizadeh, A. A. R. Darzi, and F. L. Tan, "Numerical investigations of unconstrained melting of nano-enhanced phase change material (NEPCM) inside a spherical container," International Journal of Thermal Sciences, 2012, pp. 77-83.

[14] M. Jourabian, M. Farhadi, and A. A. Rabienataj Darzi, "Outward melting of ice enhanced by Cu nanoparticles inside cylindrical horizontal annulus: Lattice Boltzmann approach," Applied Mathematical Modelling, 2013, pp. 8813-8825.

[15] J. Khodadadi and Y. Zhang, "Effects of buoyancy-driven convection on melting within spherical containers," International Journal of Heat and Mass Transfer, 2001, pp. 1605-1618.

[16] N. Wakao and S. Kaguei, "Heat and Mass Transfer in Packed BedsGordon and Breach Science Publications," New York, 1982.